Journal of Medical Diagnostic Methods
ISSN: 2168-9784

Uchida, J Med Diagn Meth 2015, 4:3
DOI: 10.4172/2168-9784.1000.178

Research Article Open Access

Evaluation of High-quality Hepatic CT Angiography with Iterative Model Reconstruction

Masafumi Uchida*

Department of Radiology, Kurume University School of Medicine, 67 Asahi-Machi, Kurume City, Fukuoka, 830-0011, Japan

***Corresponding author:** Masafumi Uchida, MD, Department of Radiology, Kurume University School of Medicine, 67 Asahi-Machi, Kurume City, Fukuoka, 830-0011, Japan, Tel: +81-942-31-7576; Fax: +81-942-32-9405, E-mail: krumf@med.kurume-u.ac.jp

Received date: Jan 27, 2015, **Accepted date:** Jul 30, 2015, **Published date:** Aug 6, 2015

Copyright: © 2015 Uchida M. This is an open-access article distributed under the terms of the Creative Commons Attribution License, which permits unrestricted use, distribution, and reproduction in any medium, provided the original author and source are credited.

Abstract

Objectives*:* To evaluate the quality of three-dimensional (3D) CT angiography images of the liver using iterative model reconstruction (IMR).

Materials and Methods: Twenty-four patients with suspected disease of the pancreatobiliary system who had undergone CT reconstruction with filtered back projection (FBP) (Protocol A), iDose (hybrid IR) (Protocol B), and IMR (Protocol C) were evaluated. Contrast-to-noise ratios (CNR) relative to the liver, aorta, and portal vein were measured and recorded. The quality of 3D images under the same CT-threshold was graded on a scale of 1 (poor) to 5 (excellent).

Results: The CNR of the artery and portal vein was highest when using protocol C. Mean value (±standard deviation) of the artery-to-liver CNRs for each protocol was as follows: A (6.95 ± 1.53), B (12.05 ± 2.38), and C (33.12 ± 7.93). Mean value (±standard deviation) of the portal vein-to-liver CNRs for each protocol was as follows: A (2.81 ± 0.62), B (5.17 ± 1.40), and C (10.27 ± 3.99). The quality of 3D images significantly differed between the three methods, with that of Protocol C being the highest.

Conclusions: Compared to FBP and hybrid IR, abdominal CT scans via IMR produced higher-quality 3D angiography images of the liver at the same radiation dose and with significant improvements in CNR.

Keywords: CT-Angiography; Liver; High-quality Iiterative model reconstruction

Introduction

The most advanced multiphase CT imaging permits a computer-simulated intra-abdominal view through body cavities and hollow viscera. Prior to surgery, this imaging provides clearer images of complicated structures than those obtained using conventional radiological examinations. CT images are the most commonly used data source for 3D images [1,2] and are of particular value when examining the liver. Studies have therefore been proposed for a planning system for surgery that utilized 3D imaging. Reliable 3D CT Angiography (CTA) rendering of the vascular anatomy of the liver aids tumor resection and laparoscopic surgery [3,4]. However, despite recent progress, resolution with abdominal CTA using a large field of view (FOV) is inferior to that with intra-arterial digital subtraction angiography (DSA), and visualization of sub-millimeter branches via CTA is relatively difficult, possibly due to depiction of small hepatic portal veins via CTA being as difficult as that of small hepatic arteries, which hampers the definitive identification of these small vessels [5,6]. A number of recent studies have focused on dose reduction and image quality when using the full IR method. In contrast, we examined thin vascular depiction using this method [7,8]. We evaluated the effect of the full iterative model reconstruction (IMR) technique on the quality of 3D CTA images of the liver.

Materials and Methods

Patient study

Twenty-four patients who underwent contrast-enhanced CT for suspected pancreatobiliary disease were enrolled. Of these patients, 18 were male and 6 female, age range was 26 to 81 years, and median age was 66 years. Data were collected over a one-year period. Definitive diagnoses included 24 pancreatobiliary lesions: cholangiocarcinoma (n=8), pancreatic carcinoma (n=6), gallbladder carcinoma (n=4), intraductal papillary mucinous tumor (n=3), focal pancreatitis (n=1), focal cholangitis (n=1), and autoimmune pancreatitis (n=1). In 14 of these patients, pancreatobiliary disease was confirmed by histology and in the other 10 by a combination of clinical course, blood chemistry test results (aspartate aminotransferase, alanine aminotransferase, alkaline phosphatase, bilirubin, albumin, and CEA antibody), and typical findings on ultrasonography, CT, and MRI. Informed consent for participation in the study was obtained from each patient or guardian as per the protocol, which was approved by the Institutional Clinical Subpanel on Human Studies at our university hospital.

CT technique

Multi-detector CT (MDCT) images were acquired using a Brilliance iCT (Philips Medical Systems, Eindhoven, the Netherlands). A slice-CT scanner at a 0.625-1.25-mm collimation setting was used to generate 0.625-1.25-mm slices, which were then reconstructed for 3D

review. Slices 0.625 mm in thickness were used for 3D imaging of arteries and 1.25 mm in thickness for portal veins. Pitch was adjusted to 1 or less when possible. Additional settings included a 30-35-cm field of view, 512 × 512 matrix size, 300-700 mA at 120 kVp, and rotation time of 0.4-0.5 sec. However, all settings depended on the physique of the patient. As these cases required thin-slice 2D and 3D CT images, the dosage was determined for each physique to decrease noise, and therefore an automatic exposure control (AEC) was not used. Scanning of the abdomen took only a few seconds. Contrast-enhanced scan for 3D CTA was conducted using a power injector (Auto Enhance A-50; Nemoto-Kyorin-Dou, Tokyo, Japan) during CTA, with contrast medium (*nonionic* iodinated *contrast* medium: iodine concentration 350 mg I/ml) injected at a rate of 4 ml/sec via a 20-gauge plastic IV catheter placed in an antecubital vein. Total volume was 630 mgI/kg with a 20 ml saline (NaCl 0.9%) flush injection. Images for each phase were obtained in the craniocaudal direction using a bolus-triggered technique by placing the cursor in the aorta and setting the CT threshold to 200 HU. The arterial phase was initiated 8 sec after 200 HU aortic enhancement time. After the arterial phase scan, the portal venous CT scan was obtained at 28 sec and hepatic venous phase CT scan at 40 sec [9].

Image processing

Three reconstruction techniques were used simultaneously: filtered back-projection (FBP) (protocol A), iDose (Hybrid IR; iDose level 5) (protocol B), and IMR (full iterative reconstruction; full IR) (protocol C).

CT Image Analysis

1: Mean CT attenuation value in Hounsfield units for the liver, aorta, and portal vein

Mean CT attenuation of the liver parenchyma, aorta and portal vein was established around the region of interest (ROI), with attempted selection of an ROI representing an area that was not small enough to be affected by pixel variability and not large enough to approach the edges of the vessel. Objective image noise was measured by obtaining the standard deviation (SD) of the mean Hounsfield unit (HU) value within a ROI.

2: Contrast-to-noise ratio (CNR)

Contrast-to-noise ratio (CNR) relative to liver for the aorta and portal vein was calculated using the following equation [10]:

$$CNR = \frac{ROI_{organ} - ROI_{background}}{\sqrt{\frac{1}{2} \times (SD_{organ}^2 + SD_{background}^2)}}$$

*organ, aorta and portal vein; background, liver parenchyma

Where: ROIorgan and ROIbackground denote the mean HU values, and SDorgan and SDbackground denote standard deviations in homogenous ROIs of the organ of interest and the surrounding background tissue, respectively.

3: 3D image quality under the same opacity curve

Images were reviewed and interpreted on an image processing workstation (ZIOSTATION2; Ziosoft, Tokyo, Japan). 3D images used volume rendering at the same opacity curve. For constant evaluation, 3D CTA images were reconstructed using all voxels higher than the selected minimum threshold of 100 HU in CT arteriography and threshold of 150 HU in CT portography. 3D images acquired via the 3 different reconstruction methods were evaluated with a visual evaluation score, ranging from 1 (poor) to 5 (excellent). Overall image quality using a 5-point scale: 5, excellent; 4, good; 3, adequate; 2, fair, of limited diagnostic value; and 1, poor, non-diagnostic (Figure 1). For scores of "excellent," sub-millimeter identification of subsegmental hepatic artery or sub-subsegmental portal branches is possible. A uniform evaluation was obtained by evaluating all cases in the same opacity curve at the same CT threshold. Qualitative image scoring of the CTA image was performed independently by two abdominal radiologists (A.S. with 14 years and Y.K. with 13 years of reading experience). In the case of disagreement between the readers, consensus was reached in a joint reading to determine the final image quality score.

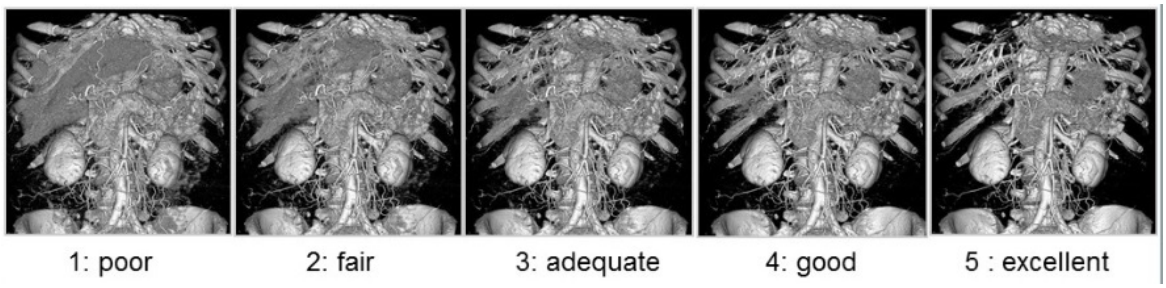

Figure 1: Evaluation figure of visual evaluation scores. Evaluation figure of visual evaluation scores. (1). In opacity curves with the same cut off CT attenuation, high level of noise decreases ease of vascular depiction and image evaluation. (2). Samples of 2D images of hepatic arterial phase of each protocol. Lowest level of noise in protocol C (IMR). Measurement of ROI with the 2D image indicates highest CNR value with protocol C (IMR). (3). Samples of 2D images of hepatic portal phase of each protocol. Lowest level of noise in protocol C (IMR). Measurement of ROI with the 2D image indicates highest CNR value with protocol C (IMR). (4). Mean 3D image quality evaluation score value. Significantly higher image quality of hepatic artery and portal vein with protocol C (IMR). (5). Samples of 3D images of hepatic arterial phase of each protocol. With the 3D image under same opacity curve, image quality of the hepatic artery was highest with protocol C (IMR), with a high CNR value and low level of noise.

Statistical Analysis

Quantitative image quality of the three protocols was compared using the Tukey-Kramer test and visual evaluation score using the Steel-Dwass test.

Results

1: Mean CT attenuation value in HU for the liver, aorta, and portal vein

Mean CT attenuation values of the liver and aorta in the arterial phase and the liver and portal vein in the portal phase are shown in Tables 1 and 2. No significant differences were observed between the three reconstruction methods. However, mean liver image noise (±SD) in the arterial phase significantly differed between Protocols A (39.55 ± 5.63), B (21.6 ± 2.56) and C (8.8 ± 1.78). Mean liver image noise (±SD) in the portal phase differed significantly between Protocols A (30.88 ± 4.92), B (15.51 ± 2.77), and C (7.55 ± 1.15).

	Mean CT attenuation	
	Liver Hus	**Aorta Hus**
Protocol A (FBP)	67.30 ± 9.91	395.45 ± 66.56
Protocol B (iDose)	66.30 ± 8.15	392.56 ± 66.68
Protocol C (IMR)	66.17 ± 6.50	398.22 ± 61.44
P-value	N.S	N.S

Table 1: Mean CT attenuation values of the liver and aorta of portal phase.

	Mean CT attenuation	
	Liver Hus	**Portal Vein Hus**
Protocol A (FBP)	107.30 ± 12.65	212.97 ± 22.99
Protocol B (iDose)	107.43 ± 12.63	213.93 ± 25.42
Protocol C (IMR)	109.69 ± 15.72	213.73 ± 20.57
P-value	N.S	N.S

Table 2: Mean CT attenuation values of the liver and portal vein of portal phase.

2: Contrast-to-noise ratio (CNR).

Mean artery-to-liver CNR and portal vein-to-liver CNR are shown in Table 3. Differences in artery-to-liver CNRs and portal vein-to-liver CNRs between the different reconstruction methods were statistically significant.

	Contrast to noise ratio	
	Artery (artery to liver CNR's)	**Portal Vein (portal vein to liver CNR's)**
Protocol A (FBP)	6.95 ± 1.53	2.81 ± 0.62
Protocol B (iDose)	12.05 ± 2.38	5.17 ± 1.40
Protocol C (IMR)	33.12 ± 7.93	10.27 ± 3.99
P-value	P<0.01	P<0.01

Table 3: Mean contrast to noise ratio (CNR) of the artery and portal Vein

3: 3D image quality under the same opacity curve

Mean evaluation scores of 3D image quality (±SD) under the same opacity curve of artery for each protocol were as follows: A (1.2 ± 0.4), B (3.1 ± 0.7), and C (4.6 ± 0.6). 3D image quality differed significantly between the three reconstruction methods, with that of Protocol C being the highest (Figure 2). Mean evaluation scores of 3D image quality (±SD) under the same opacity curve of portal vein for each protocol were as follows: A (2.7 ± 0.7), B (3.9 ± 0.7), and C (4.8 ± 0.7). Three-dimensional image quality differed significantly between the three reconstruction methods, with that of Protocol C (IMR) being the highest.

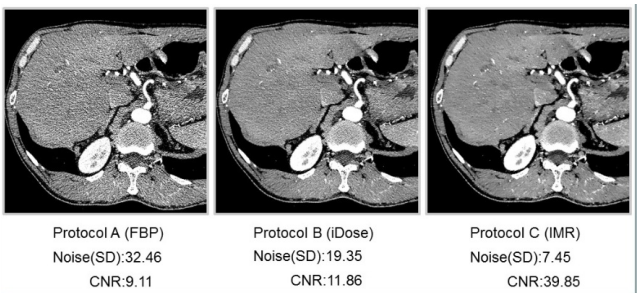

Figure 2: Samples of 2D images of hepatic arterial phase of each protocols. Samples of 3D images of hepatic portal phase of each protocol. (6). With the 3D image under same opacity curve, image quality of the hepatic portal vein was highest with protocol C (IMR), with a high CNR value and low level of noise. (7). 3D-CTA of 48-year-old female with pancreas intraductal papillary mucinous tumor with suitable cut-off CT threshold CT threshold at lowest setting in optimal opacity curve in Protocol C (IMR) and highest quality 3D CTA. High CNR and low noise obtained in Protocol C (IMR) with low CT threshold are preferable for high-quality 3D CTA. Low level of noise to reduce the vascular threshold is preferable. Subsegmental hepatic arteries are found clearly in Protocol C. (8). 3D-CTA of a 69-year-old man with pancreatic carcinoma with suitable cut-off CT threshold Cut-off CT threshold at lowest setting in optimal opacity curve in protocol C (IMR) and highest quality 3D CTA. High CNR and low noise obtained in protocol C (IMR) with low cut-off CT threshold are preferable for high-quality 3D CTA. Sub subsegmental portal branches are found clearly in protocol C.

Discussion

The recent introduction of MDCT scanners for abdominal imaging has enabled the acquisition of optimal dynamic images with high temporal and z-axis resolution. MDCT also enables the comprehensive evaluation of CTA. In abdominal vessels, 3D CTA is now a suitable diagnostic procedure for disorders of the liver and its major branches [11,12]. In the evaluation of abdominal veins, 3D CT portography and venography are effective in the depiction of hepatic portal venous anatomy [13]. Recently, several manufacturers have introduced new

CT reconstruction algorithms based on iterative rather than traditional filtered back-projection (FBP) reconstruction [14,15]. Iterative reconstruction (IR) algorithms provide superior image quality on CTA, mainly due to reduced image noise and improved CNR. These IR algorithms might be more efficient than FBP, and manufacturers have proposed that they decrease radiation dose while maintaining comparable image quality to standard-dose FBP CT [10,16]. However, image reconstruction was performed using the hybrid IR method, in which IR and FBP techniques are combined. The recently developed full IR method is the newest IR method and ensures complete reconstruction, providing even greater noise reduction and improving both spatial and low-contrast resolution [17,18]. However, while some studies have reported dose reduction using the full IR method, to our knowledge [17], ours is the first to report the utility of 3D CTA using the full IR method with the same CT threshold in the same opacity curve.

Volume-rendering processing is a recently developed 3D imaging technique [19,20]. One factor that is essential for CTA volume-rendering processing is the opacity curve with a cut-off CT attenuation value. Adequate contrast enhancement and optimal opacity determination will produce homogeneous and high-quality 3D images. Minimization of the cut-off CT threshold improves thin vascular depiction. However, under the same opacity curve with same CT threshold, thin vascular depiction is difficult with low CNR and high noise. Large decreases in CT threshold result in increases in perivascular noise, which disturbs imaging. High-quality CTA for the depiction of thin vessels therefore requires images with high CNR and a low level of noise. Upon examination of image quality, an optimal IMR method with high CNR and a low level of noise was obtained. With our new protocol, high-resolution CTA with full iterative reconstruction produces high-quality images with high CNR and a low level of noise. In addition, imaging of sub-millimeter-diameter vessels might also be possible. High-resolution 3D CTA imaging raises the possibility of aligning accurate and detailed anatomical information of the hepatobiliary pancreatic system with spatial data provided by MD-CT. For evaluation of image quality under the same condition in this examination, the CT threshold and opacity curve were also the same. The most suitable CT threshold is selected for each case and 3D CTA then conducted. Figure 2 are images of CTA with the most suitable CT threshold. When CNR is high and noise is low, the setting for the cut-off CT threshold can be low and 3D CTA conducted. Using this approach, the lowest cut-off CT threshold in IMR can be obtained.

A limitation to the present study warrants mention. The study was conducted using standard doses as many studies of the IR method using lower doses provided images with quality equal to standard CT. Therefore, the depiction of thin vessels might be possible using the full IR method with a standard dose. Further investigation using CTA imaging at low doses is required to confirm these results.

In conclusion, evaluation of abdominal CT scans via full IR produced higher quality 3D CTA images of the liver with the same radiation dose and a significant decrease in noise and CNR than FBP and hybrid IR.

References

1. Schroeder T, Radtke A, Kuehl H, Debatin F, Malago M, et al. (2006) Evaluation of Living Liver Donorswith an All-inclusive 3D Multi-Detector Row CT Protocol. Radiology 238: 900-910.
2. Uchida M (2014) Recent advances in 3D computed tomography techniques for simulation and navigation in hepatobiliary pancreatic surgery. J Hepatobiliary Pancreat Sci 21: 239-245.
3. Saito S, Yamanaka J, Miura K, Nakao N, Nagao T, et al. (2005) A Novel 3D Hepatectomy Simulation Based on Liver Circulation: Application to Liver Transplantation. HEPATOLOGY 41: 1297-1304.
4. Beller S, Hünerbein M, Eulenstein S, Lange T, Schlag PM (2007) Feasibility of Navigated Resection of Liver Tumors Using Multiplanar Visualization of Intraoperative 3-dimensional Ultrasound Data, Ann Surg 246: 288-294.
5. Mollet NR, Cademartiri F, van Mieghem CA, Runza G, McFadden EP, et al. (2005) High-Resolution Spiral Computed Tomography Coronary Angiography in Patients Referred for Diagnostic Conventional Coronary Angiography. Circulation 112: 2318-2323.
6. Villablanca JP, Rodriguez FJ, Stockman T, Dahliwal S, Omura M, et al. (2007) MDCT Angiography for Detection and Quantification of Small Intracranial Arteries: Comparison with Conventional Catheter Angiography. Am J Roentgenol 188: 593-602.
7. Perry JP, Meghan GL, Lubner DHK (2012) Abdominal CT With Model-Based Iterative Reconstruction (MBIR): Initial Results of a Prospective Trial Comparing Ultralow-Dose With Standard-Dose Imaging. Am J Roentgenol 199: 1266-1274.
8. Deák Z, Grimm JM, Treitl M, Geyer LL, Linsenmaier U, et al. (2013) Filtered Back Projection, Adaptive Statistical Iterative Reconstruction, and a Model-based Iterative Reconstruction in Abdominal CT: An Experimental Clinical Study. Radiology 185-196.
9. Uchida M, Sakoda J, Arikawa (2009) Comparison of Dynamic MRI at 3.0 T and MDCT of the Pancreatobiliary System: Initial Comprehensive Evaluation with Source, MPR, CPR Images and Angiographic Reconstructions. JMRI 29: 846-852.
10. Utsunomiya D, Weigold WG, Weissman G, Taylor AJ (2012) Effect of hybrid iterative reconstruction technique on quantitative and qualitative image analysis at 256-slice prospective gating cardiac CT. Eur Radiol 22: 1287-1294.
11. Suzuki H, Oshima H, Shiraki N, Ikeya C, Shibamoto Y. (2004) Comparison of two contrast materials with different iodine concentrations in enhancing the density of the the aorta, portal vein and liver at multi-detector row CT: a randomized study. Eur Radiol 14: 2099-2104.
12. Ichikawa T, Motosugi U, Morisaka H, Sou H, Onohara K, et al. (2012) Optimal iodine dose for 3-dimensional multidetector-row CT angiography of the liver. Eur J Radiol 81: 2450-2455.
13. Uchida M, Ishibashi M, Sakoda J, Azuma S, Nagata S, et al. (2007) CT image fusion for 3D depiction of anatomic abnormalities of the hepatic hilum. Am J Roentgenol 189: 184-191.
14. Willemink MJ, Leiner T, de Jong PA, de Heer LM, Nievelstein RA, et al. (2013) Iterative reconstruction techniques for computed tomography part 2: initial results in dose reduction and image quality. Eur Radiol 23: 1632-1642.
15. Hara AK, Paden RG, Silva AC, Kujak JL, Lawder HJ, Pavlicek W (2009) Iterative Reconstruction Technique for Reducing Body Radiation Dose at CT: Feasibility Study. Am J Roentgenol 193: 764-771.
16. Singh S, Kalra MK, Hsieh J, Licato PE, Do S, et al. (2010) Abdominal CT: Comparison of Adaptive Statistical Iterative and Filtered Back Projection Reconstruction Techniques. Radiology 257: 373-383.
17. Pickhardt PJ, Lubner MG, Kim DH, Tang J, Ruma JA, et al. (2012) Abdominal CT With Model-Based Iterative Reconstruction (MBIR): Initial Results of a Prospective Trial Comparing Ultralow-Dose With Standard-Dose Imaging. Am J Roentgenol 199: 1-9.
18. Löve A, Olsson ML, Siemund R, Stålhammar F, Björkman-Burtscher IM, et al. (2013) Six iterative reconstruction algorithms in brain CT: a phantom study on image quality at different radiation dose levels. Br JRadiol 86: 1031-1042.
19. Schroeder T, Radtke A, Kuehl H, Debatin JF, Malagó M, et al. (2006) Evaluation of Living Liver Donors with an All-inclusive 3D Multi-Detector Row CT Protocol. Radiology 238: 900-910.

20. Sugimoto M, Yasuda H, Koda K, Suzuki M, Yamazaki M, et al. (2010) Image overlay navigation by markerless surface registration in gastrointestinal, hepatobiliary and pancreatic surgery. J Hepatobiliary Pancreat Sci 17: 629-636.